Geosciences Faculty Publications   Department of Geosciences

2020

Oxygen Isotopes in Authigenic Clay Minerals: Toward Building a Reliable Salinity Proxy

Daniel Gebregiorgis

Daniel M. Deocampo

Fred Longstaffe

A. Simpson

Gail M. Ashley

See next page for additional authors

Authors

Daniel Gebregiorgis, Daniel M. Deocampo, Fred Longstaffe, A. Simpson, Gail M. Ashley, Emily Beverly, Jeremy Delaney, and Javier Cuadros

Here we report the first quantitative reconstruction of salinity changes in paleolake Olduvai based on oxygen-isotope measurements of authigenic clay minerals and the relationship between TDS (total dissolved solids) and the oxygen isotope composition of lake water at Ngorongoro Crater (Deocampo, 2001; Deocampo, 2004). Based on this isotopic record, we examine the orbital forcing mechanism of the East African monsoon system during the warm periods of the early Pleistocene (~1800–1920 kyr), a key interval in Quaternary paleoclimate and the evolution of the hominin lineage (Trauth et al., 2005).

During the early Pleistocene, the Olduvai basin covered ~3,500 km^2 and had a perennial, saline, alkaline lake near its center. Samples for this study were collected between two chronostratigraphic markers, Tuffs IB and IIA, representing ~110 kyr spanning the upper portion of Bed I and lowermost Bed II (Deino, 2012). The Plio-Pleistocene deposits are composed mostly of reworked volcaniclastic sediment with most of the central basin deposits being authigenic precipitates or alteration products (Hay, 1976). In the saline, alkaline, and silica-rich waters of many East African lakes, authigenic clay minerals can become enriched in octahedral Mg relative to the Al-rich clays produced either within the lakes during periods of lower salinity or outside the lakes and washed in as detrital sediment (Deocampo, 2015). Clay minerals form in isotopic equilibrium with ambient water at the time of crystallization; the magnitude of the clay-water oxygen-isotope fractionation is controlled primarily by clay mineral composition, structure, and water temperature (Savin & Lee, 1988). Once formed, the oxygen atoms in tetrahedral and octahedral sheets are fixed and do not exchange with pore fluids unless further dissolution-precipitation reactions occur (e.g., through burial diagenesis). Therefore, the isotopic signature of authigenic lacustrine clay minerals can be related to the isotopic composition of paleo-waters, and hence to paleosalinity driven by evaporation.

Interannual variability of rainfall in East Africa is influenced by complex interactions among topography, sea surface temperature (SST) forcing, large-scale ocean-atmosphere teleconnections (e.g., El Niño–Southern Oscillation = ENSO), and features associated with synoptic-scale weather systems such as tropical cyclones both north (e.g., Gebregiorgis et al., 2019) and south of the equator (e.g., Otte et al., 2017). The distribution of rainfall in East Africa, however, is closely connected to the north-south displacement of the African Rain belt, also widely cited in a variety of scientific literature as the Intertropical Convergence Zone or ITCZ (Nicholson, 2018). The tropical African rain belt oscillates north and south of the equator with the seasonal march of the Sun and determines the seasonality of rainfall across the region (i.e., December-February in the Southern Hemisphere, SH, and June-September in the Northern Hemisphere, NH) (Figures 1a and 1b). This variability is reflected in the oxygen-isotope patterns of precipitation in the region, with lowest δ^{18}O occurring during the two rainy seasons (Rozanski et al., 1996). The isotopic signal captured by authigenic clay minerals are then controlled by the duration and intensity of monsoon inflows, and subsequent evaporative concentration under hydrologically closed conditions. If the clay mineralogy, water paleotemperature, and preevaporative isotopic composition of the meteoric water that supplied the lake are all well constrained, then the oxygen-isotope composition of clay minerals can be used as a direct indicator of evaporative concentration and salinity in a lake (Skrzypek et al., 2015) and therefore monsoon intensity.

2. Materials and Methods

Thirty-nine (39) samples were selected for clay mineral purification and subsequent oxygen-isotope analysis, based on their stratigraphic position within the upper portion of Bed I and lowermost Bed II, spanning the age range ~1780–1910 kyr (Deino, 2012). The age model is based on linear interpolation between dated tuffs (I-F, I-B, and I-A) following Hay and Kyser (2001) and using a new ^{40}Ar/^{39}Ar and paleomagnetic chronology (Deino, 2012; Deocampo et al., 2017). Analysis of these tuffs yield dates of 1.803 $\pm$ 0.002, 1.848 $\pm$ 0.003, and 1.92 $\pm$ 0.003 Myr, respectively. Sediment ages between the tie points were linearly interpolated. Ultrafine clay size-fractions (<0.1 μm) were separated from the bulk sediments following routine centrifugation protocols (Moore & Reynolds, 1997), and their clay mineralogy determined by X-ray diffraction (XRD). Samples were analyzed in air-dried and ethylene-glycolated states using Cu-Kα radiation from 3 to 35° 2θ, following Moore and Reynolds (1997). Details of the instrumental parameters employed can be found in Deocampo et al. (2009) and Simpson (2016).

Oxygen-isotope analyses were performed at the University of Western Ontario following Libbey et al. (2013) and references therein. Reproducibility was better than ±0.2‰. Paleolake salinity was determined based on
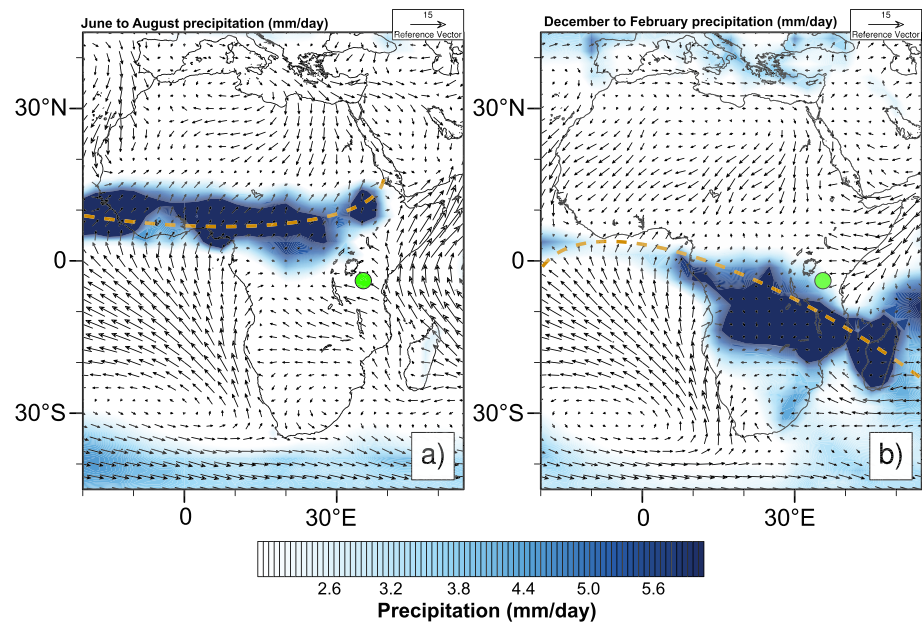
Figure 1. Changes in seasonal mean precipitation and surface wind vectors in East Africa. (a) June-August, and (b) December-February mean precipitation (mm/day) for the period 1979–2015 (GPCC precipitation data provided by the NOAA/OAR/ESRL PSD and can be accessed at https://www.esrl.noaa.gov/psd/). The green circle shows the location of the Olduvai Gorge. Broken lines show the approximate locations of the tropical rain belt during the same months.

paired measurements of modern $\delta^{18}O_{LW}$ and TDS for meteoric surface water at Ngorongoro Crater (Deocampo, 2001; Deocampo, 2004) where TDS = $(0.3 \times \delta^{18}O_{LW}) + 1.64$.

3. Results and Discussions

3.1. Clay Mineralogy

XRD showed that the <0.1 μm clay fraction was dominated by illite, smectite, and interstratified illite-smectite. The percentages of illitic and smectitic layers were determined based on detailed study of glyco-lated, oriented clay mounts. For mixtures of smectite and illite end-members, their relative abundances were estimated by comparison of peak intensity of basal diffractions (Carroll, 1970). For samples containing inter-stratified illite-smectite, proportions of illite and smectite layers were determined by the Δ2θ method of Moore and Reynolds (1997). Samples varied from illite-rich to smectite-rich while interstratified illite-smectite was common (Simpson, 2016). Identifiable illite is present in 33 of 39 samples. The smectite-rich samples show strong 001 peaks at ~1.70 nm due to the swelling behavior of smectite that causes expansion of the interlayer space in glycolated mounts (Figure 2). Air-dried and glycolated patterns are identical for all pure illite phases, with 001 diffractions at ~1.0 nm and 002 diffractions at ~0.5 nm (Figure 2). The maximum
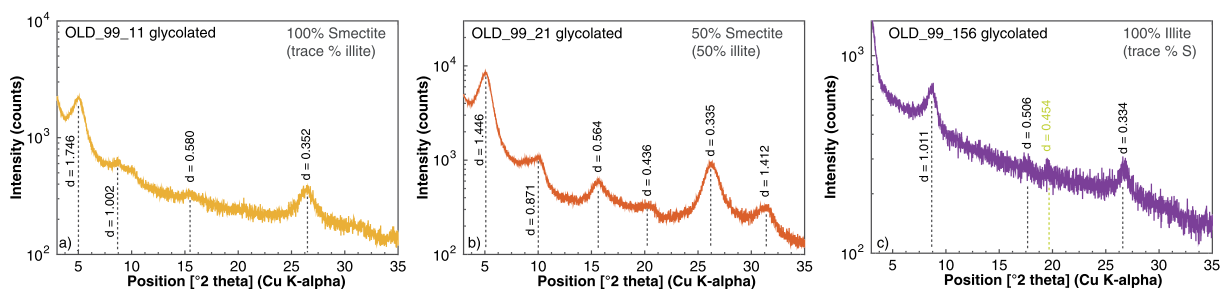
Figure 2. XRD patterns of glycolated mounts of typical authigenic clays from Olduvai: (a) Sample OLD_99_11, (b) Sample OLD_99_21, and (c) Sample OLD_99_156. The d-spacing (nm) of each peak is provided. Trace of illite in (a) is indicated by the 1 nm peak. The illite XRD pattern in (c) shows the 020 peak maximum at 0.454 nm, indicating that illite is trioctahedral (i.e., Mg-rich).

AGU
100
ADVANCING EARTH
AND SPACE SCIENCE

Geophysical Research Letters

10.1029/2019GL085576

at 0.454 nm in Figure 2c is the 020 diffraction and indicates that the illite is trioctahedral, or Mg-rich (Cuadros et al., 2013). This finding is confirmed by 060 peak measurements for the same and similar samples in randomly oriented powder preparations, with strong 060 peaks at ~0.152 nm (Simpson, 2016). These results confirm the authigenic origin of this illite. These results are consistent with previous microtextural and high-resolution geochemical studies showing that the <0.1 μm size-fraction of central basin clays is dominated by neoformed, authigenic clay minerals (Deocampo et al., 2009; Deocampo et al., 2017; Hay & Kyser, 2001; Hover & Ashley, 2003).

3.2. Isotopic Fractionation in Authigenic Clay Minerals

The complexities and multiple modes of low-temperature illitization of smectite remain an active area of research that holds important implications for understanding settings such as Olduvai. Although complete dissolution-precipitation is well documented for some Olduvai authigenic clay minerals, Deocampo et al. (2009) found high-resolution transmission electron microscopy (TEM) evidence for both dissolution-precipitation and layer-by-layer transformation in the process of smectite illitization, even within the same samples. Our results suggest that layer-by-layer transformation producing part of the illite layers did not inhibit oxygen-isotope equilibration between illite layers and lake water. First, all illite layers generated by dissolution-precipitation had full opportunity for complete oxygen-isotope exchange with water to occur. Second, layer-by-layer illitization would also fully replace the anionic component of the layers ("reacting interlayer" model of Altaner & Ylagan, 1997), again facilitating complete oxygen-isotope exchange.

We used the clay-water oxygen-isotope geothermometers for illite, smectite, and interstratified illite-smectite (Savin & Lee, 1988) to estimate lake water oxygen-isotope compositions. Equation (1) describes this relationship for illite-smectite:

$$1,000 \times \ln\alpha^{ox}_{[illite-smectite]-water} = (2.58 - 0.19*I)*10^6 \, T^{-2} - 4.19 \tag{1}$$

In equation (1), α^{ox} is the oxygen-isotope fractionation factor between illite-smectite and water, "I" is the decimal fraction of illitic layers in the mixed-layer illite-smectite, and T is temperature in Kelvin. The same <0.1 μm clay separates, for which illite, smectite, and interstratified illite-smectite abundances were determined by XRD, were analyzed for their oxygen-isotope compositions.

Using the above understanding of isotopic fractionations between paleolake water and authigenic clay minerals, we propose a model of proxy development as shown in Figure 3. The closed-system batch model has three steps, using the major ion and oxygen-isotope compositions of dilute waters of northern Tanzania as a starting point (Deocampo, 2001; Deocampo, 2004). Although the model does not capture some of the mass loss due to early carbonate precipitation, that effect is trivial compared to the bulk of conservative dissolved solids (Deocampo & Jones, 2014; Deocampo & Renaut, 2016). First, the model predicts the change in TDS that would result from 50% water volume loss ("humid" conditions, Figure 3a) versus 95% loss ("arid" conditions, Figure 3b) during evaporation. Second, based on the modern calibration data set, the model calculates $\delta^{18}O_{lake\ water}$. Third, it applies the mineral water fractionation factors as discussed above to determine the $\delta^{18}O_{clay}$, assuming 50% smectite layers and 50% illite layers. Based on these calculations (that are only valid for the assumed conditions), $\delta^{18}O_{clay}$ is predicted to range between ~ +20 and +26‰, values similar to the limited data previously available for authigenic clays from paleolake Olduvai (Hay & Kyser, 2001).

Application of equation (1) requires that lake water temperature is known or can be reasonably well constrained. Today, mean annual temperatures at Olduvai Gorge are ~25 °C. Here we have calculated $\alpha^{ox}_{[illite-smectite]\ -\ water}$ for a slightly wider temperature envelope (24–26 °C). Using the isotopic compositions measured for structural oxygen in the authigenic clay ($\delta^{18}O_C$), we then solved for lake water oxygen-isotope compositions ($\delta^{18}O_{LW}$). The range obtained for $\delta^{18}O_{LW}$ is consistent with ground water $\delta^{18}O$ measurements from near Lake Naivasha (Ojiambo et al., 2001).

3.3. Early Pleistocene Pacing of the East African Monsoon Based on a New Salinity Proxy

Our ability to reconstruct past continental climatic and hydrological changes is hampered by the lack of reliable proxies for key paleoecological parameters such as salinity. The key finding of this study, as detailed below (Figure 4), is that the timing and relative amplitude of $\delta^{18}O_{LW}$ and salinity changes in paleolake
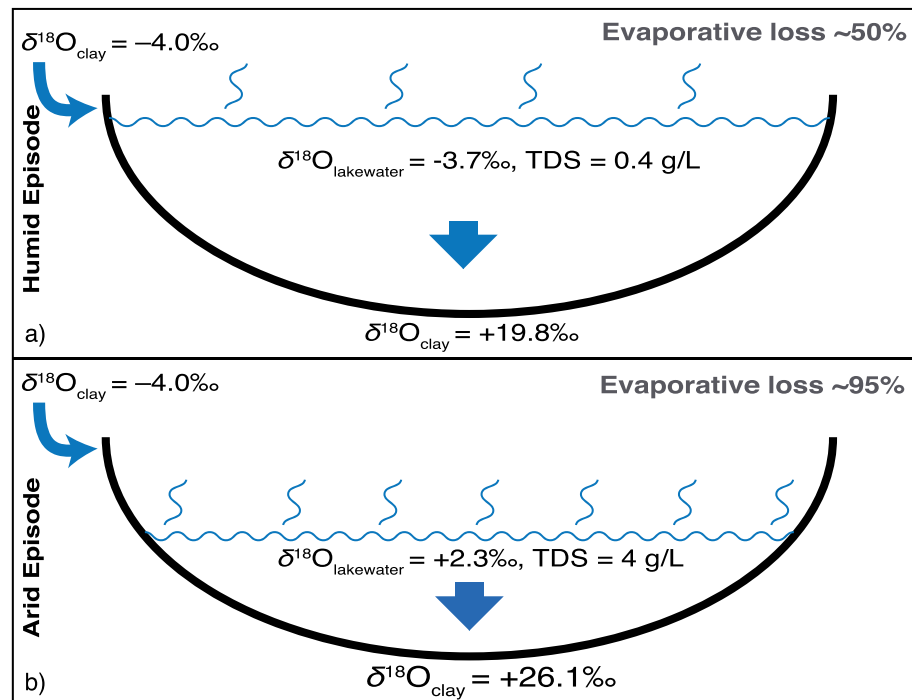
Figure 3. Schematic model for the clay mineral oxygen-isotope proxy for paleosalinity. Evaporative concentration leads to ^{18}O-enrichment of residual lake water, which in turn increases the $\delta^{18}O$ of authigenic clays formed in the lake. Model calculations were based on the following: (1) $\delta^{18}O_{inflow}$ = −4.0‰ (VSMOW); (2) dilute inflow total dissolved solids (TDS) = 0.2 g/L (Deocampo, 2004); (3) the relationship between TDS and oxygen-isotope fractionation following evaporative concentration follows modern observations in the region [TDS = (0.3 × $\delta^{18}O_{lake\ water}$) + 1.64] (Deocampo, 2001, 2002, 2004); and (4) authigenic clay sedimentation is in the form of interstratified illite-smectite with 50% illite layers, according to equation (1) (Savin & Lee, 1988).

Olduvai were controlled by changes in monsoon intensity. In order to evaluate the validity of $\delta^{18}O_{LW}$ as a salinity proxy, we compared the $\delta^{18}O_{LW}$ record with freshwater stages identified by high whole-rock Al_2O_3/MgO ratios (Deocampo et al., 2017) and records of $\delta^{13}C$ indicating ecosystem changes at Olduvai (Magill et al., 2013) (Figure 4). The paleoecological record of $\delta^{13}C$ of leaf waxes varies systematically, but appears to be nonlinearly related to geochemical signals of aridity, as also found by Magill et al. (2013). This pattern may reflect C4 overrepresentation due to taphonomic processes as well as inherent biases in the leaf wax record toward wet climates (Post-Beittenmiller, 1996; Wynn, 2007). Deocampo et al. (2017) suggested that the composition of Olduvai clays is mediated by the prevailing climate conditions in the region. Accordingly, Al-rich clays are more likely to have formed during increased lake freshening and strengthened monsoon intensity while the opposite is the case for Mg-rich clays. Our results show that during the early Pleistocene, $\delta^{18}O_{clay}$ varied from +20.2 to +26.2‰, with reconstructed paleolake $\delta^{18}O_{LW}$ ranging from about −2.7 to +2.9‰ (VSMOW). This variation corresponds to paleolake salinities (TDS) of ~0.2 to 2.7 g/L. These values are typical for saline, alkaline lakes of East Africa, reflecting moderate to significant evaporative concentration in a hydrologically closed basin (Deocampo & Renaut, 2016).

Reconstructed $\delta^{18}O_{LW}$ and paleolake salinity are consistent with records of $\delta^{13}C$ indicating ecosystem changes at Olduvai (Magill et al., 2013). While the pattern of dry/wet (saline/fresh) oscillations identified based on the $\delta^{18}O_{LW}$ record and the whole-rock Al_2O_3/MgO are broadly similar, however, the absolute ages of dry/wet conditions revealed by the whole-rock Al_2O_3/MgO ratios and reconstructed paleolake salinity disagree (Figure 4). We also identify a long-term trend toward lower salinity from ~1830–1920 kyr that is not evident in the other proxy records (Figure 4, middle). This coincides with a time interval when tropical SSTs were relatively warmer (Figure 4, top, Hebert et al., 2010). Superimposed on this wetting trend, the paleolake salinity record reveals several dry-wet (weak/strong monsoon) oscillations. Taken at face value, the data appear to imply a temporal link between precession and changes in monsoon intensity with four
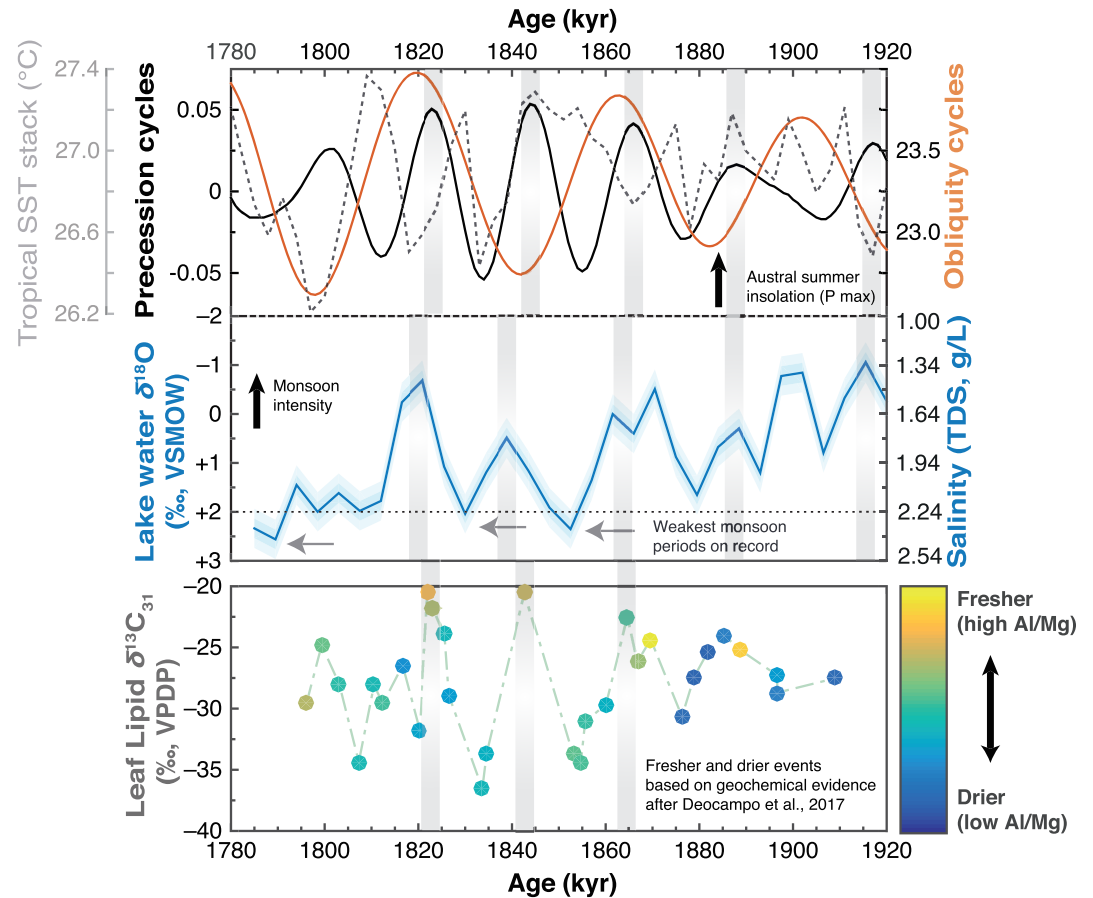
Figure 4. Quantitative reconstruction of paleolake salinity: (top) Earth's obliquity and precession cycles shown together with a high-resolution tropical SST stack (°C) after Herbert et al. (2010). The tropical SST stack is constructed based on four alkenone-based SST reconstructions from tropical Pacific Ocean, South China Sea, Arabian Sea, and Tropical Atlantic Ocean: (middle) Changes in reconstructed lake water oxygen-isotope composition ($\delta^{18}O_{LW}$) on evenly spaced (linearly interpolated) time axis running from ~1780 to 1920 kyr in 4.5 kyr intervals and derived paleolake salinity, and (bottom) leaf lipid $\delta^{13}C_{31}$ records documenting ecosystem changes at Olduvai. The blue envelops show the range of $\delta^{18}O_{LW}$ calculated for 24 to 26 °C. The leaf lipid $\delta^{13}C_{31}$ include a code color indication of aridity as determined by a geochemical indicator (whole-rock Al_2O_3/MgO) from the same site (Deocampo et al., 2017). Note that the paleoecological record of $\delta^{13}C$ of leaf waxes varies systematically, but appears nonlinearly related to geochemical signals of aridity.

major freshening events in-phase with maximum precession. Also note that three major freshening events also coincide with periods of maximum obliquity. The divergence between the salinity record and those of precession between ~1860 and 1900 kyr (Figure 4), however, suggests that salinity changes are not linearly related to changes in precessional or obliquity cycles. For example, maximum wetness intervals centered at ~1900 and ~1915 Kyr occur when precession-driven local insolation changes at Olduvai are relatively muted (Laskar et al., 2004). Given the long-term trend toward lower salinity and tropical SST warming from ~1830–1920 kyr, fluctuations in monsoon intensity during the same interval are not simply related to orbitally induced changes in insolation (Figure 4). Early Pleistocene pacing of the East African monsoon when precession variability was relatively muted was therefore likely driven by changes in tropical SSTs rather than direct insolation.

Such a scenario is consistent with the monsoon response to the ENSO or Indian Ocean dipole (IOD) cycles where warmer conditions in the equatorial Pacific and western Indian Oceans (i.e., a positive IOD state) induce strong monsoons over tropical eastern African in addition to the north-south displacement of the tropical African rain belt (e.g., Behera et al., 2005). Modern observations show that the East African monsoon

system is sensitive to changes in the Walker Circulation regulated by ENSO and IOD. Modeling studies show that changes in orbital configurations influence tropical Pacific mean climate by increasing or decreasing insolation over the tropics (e.g., Clement et al., 1999; Lu et al., 2019; Shi et al., 2012; Timmermann et al., 2007). For example, as precession reaches maxima (i.e., at maximum austral summer insolation and when NH summer solstice occurs near the aphelion—the point in the orbit of the Earth farthest away from the Sun), the SST in eastern tropical Pacific is significantly warmer in the models and an El Niño-like condition prevails (e.g., Shi et al., 2012). The opposite scenario (i.e., minimum precession) results in a La Niña-like condition (e.g., Clement et al., 1999; Shi et al., 2012; Timmermann et al., 2007). Changes in the tilt of the Earth or obliquity are also shown to influence the tropical Pacific mean climate and annual mean insolation over the central eastern equatorial Pacific (e.g., Lu et al., 2019). Therefore, one cannot always expect the East African monsoon system to consistently follow latitudinal changes in insolation and the predicted North–South migration of the tropical African rain belt. In view of these results, transient model simulations are needed to better understand the nonlinear response of the East African monsoon to insolation changes triggered by Earth's precessional and obliquity cycles. Such an approach may better accommodate evidence for a greater role of tropical warming at peak precession and obliquity.

4. Conclusions and Implications

Developing a quantitative proxy for salinity—a key paleoecological parameter in hydrologically closed continental basins—has been elusive, especially where microfossils are absent. The first clay mineral oxygen-isotope time series from Olduvai Gorge provides evidence that such data can be used as a direct indicator of lake water salinity. We observe significant salinity changes in the basin between ~1800 and 1920 kyr. These changes are strongly in phase with maximum orbital precession. A closer look at the data, however, suggests that the increase or decrease in East African monsoon intensity is not simply related to changes in NH insolation. Instead, we conclude that the early Pleistocene pacing of the East African monsoon may have also been controlled by SST changes in the tropical oceans and weakening/strengthening of the Walker circulation. While the sensitivity of authigenic clay mineral oxygen-isotope compositions to nonenvironmental factors needs to be explored in greater detail, we anticipate that such factors will be minor relative to the differences reported here. Even if the sensitivity of oxygen-isotope data needs to be further investigated, the present results are very encouraging and provide a firm foundation for paleosalinity reconstructions in other East African lake sites.

References

Altaner, S. P., & Ylagan, R. F. (1997). Comparison of structural models of mixed-layer illite/smectite and reaction mechanisms of smectite illitization. *Clays and Clay Minerals*, *45*(4), 517–533. https://doi.org/10.1346/CCMN.1997.0450404

Behera, S. K., Luo, J. J., Masson, S., Delecluse, P., Gualdi, S., Navarra, A., & Yamagata, T. (2005). Paramount impact of the Indian Ocean dipole on the East African short rains: A CGCM study. *Journal of Climate*, *18*(21), 4514–4530. https://doi.org/10.1175/JCLI3541.1

Carroll, D. (1970). Clay minerals: A guide to their X-ray identification. Geological Society of America Special Paper 126, Boulder, Colorado, USA.

Chevalier, M., Brewer, S., & Chase, B. M. (2017). Qualitative assessment of PMIP3 rainfall simulations across the eastern African monsoon domains during the mid-Holocene and the Last Glacial Maximum. *Quaternary Science Reviews*, *156*, 107–120. https://doi.org/10.1016/j.quascirev.2016.11.028

Clement, A. C., Seager, R., & Cane, M. A. (1999). Orbital controls on the El Nino/Southern Oscillation and the tropical climate. *Paleoceanography*, *14*(4), 441–456. https://doi.org/10.1029/1999PA900013

Cuadros, J., Michalski, J. R., Dekov, V., Bishop, J., Fiore, S., & Dyar, M. D. (2013). Crystal chemistry of interstratified Mg/Fe-clay minerals from seafloor hydrothermal sites. *Chemical Geology*, *360*, 142–158. https://doi.org/10.1016/j.chemgeo.2013.10.016

Deino, A. L. (2012). ^{40}Ar/^{39}Ar dating of Bed I, Olduvai Gorge, Tanzania, and the chronology of early Pleistocene climate change. *Journal of Human Evolution*, *63*(2), 251–273. https://doi.org/10.1016/j.jhevol.2012.05.004

Deocampo, D. M. (2001). Geochemistry and sedimentology of modern East African wetlands and a Pleistocene paleo-wetland at Olduvai Gorge, Tanzania: Ph.D. thesis, Rutgers University, 155 p.

Deocampo, D. M. (2002). Sedimentary processes and lithofacies in lake-margin groundwater-fed wetlands in East Africa. In R. W. Renaut & G. M. Ashley (Eds.), *Sedimentation in Continental Rifts* (Vol. 73, pp. 295–308). Tulsa, OK: Society for Sedimentary Geology (SEPM) Special Publication.

Deocampo, D. M. (2004). Hydrogeochemistry in the Ngorongoro Crater, Tanzania, and implications for land use in a world heritage site. *Applied Geochemistry*, *19*(5), 755–767. https://doi.org/10.1016/j.apgeochem.2003.10.006

Deocampo, D. M. (2015). Authigenic clay minerals in lacustrine mudstones. *Geological Society of America Special Papers*, *515*, SPE515–03.

Deocampo, D. M., Berry, P. A., Beverly, E. J., Ashley, G. M., & Jarrett, R. E. (2017). Whole-rock geochemistry tracks precessional control of Pleistocene lake salinity at Olduvai Gorge, Tanzania: A record of authigenic clays. *Geology*, *45*(8), 683–686. https://doi.org/10.1130/G38950.1

Deocampo, D. M., Cuadros, J., Wing-Dudek, T., Olives, J., & Amouric, M. (2009). Saline lake diagenesis as revealed by coupled mineralogy and geochemistry of multiple ultrafine clay phases: Pliocene Olduvai Gorge, Tanzania. *American Journal of Science*, *309*(9), 834–868. https://doi.org/10.2475/09.2009.03

Deocampo, D. M., & Jones, B. F. (2014). Geochemistry of saline lakes. *Treatise on Geochemistry*, *7*, 437–469. https://doi.org/10.1016/B0-08-043751-6/05083-0

Deocampo, D. M., & Renaut, R. W. (2016). *Geochemistry of African soda lakes: In M. Schagerl (Ed.), Soda lakes of East Africa* (pp. 77–93). Springer International, Cham.

Gebregiorgis, D., Rayner, D., & Linderholm, H. W. (2019). Does the IOD independently influence seasonal monsoon patterns in northern Ethiopia? *Atmosphere*, *10*(8), 432. https://doi.org/10.3390/atmos10080432

Hay, R., & Kyser, T. (2001). Chemical sedimentology and paleoenvironmental history of Lake Olduvai, a Pliocene lake in northern Tanzania. *Geological Society of America Bulletin*, *113*(12), 1505–1521. https://doi.org/10.1130/0016-7606(2001)113<1505:CSAPHO>2.0.CO;2

Hay, R. L. (1976). *Geology of the Olduvai Gorge*. Berkeley, CA: University of California Press.

Herbert, T. D., Peterson, L. C., Lawrence, K. T., & Liu, Z. (2010). Tropical ocean temperatures over the past 3.5 million years. *Science*, *328*(5985), 1530–1534. https://doi.org/10.1126/science.1185435

Hover, V. C., & Ashley, G. M. (2003). Geochemical signatures of paleodepositional and diagenetic environments: A STEM/AEM study of authigenic clay minerals from an arid rift basin, Olduvai Gorge, Tanzania. *Clays and Clay Minerals*, *51*(3), 231–251. https://doi.org/10.1346/CCMN.2003.0510301

Laskar, J., Robutel, P., Joutel, F., Gastineau, M., Correia, A. C. M., & Levrard, B. (2004). A long-term numerical solution for the insolation quantities of the Earth. *Astronomy & Astrophysics*, *428*(1), 261–285. https://doi.org/10.1051/0004-6361:20041335

Libbey, R. B., Longstaffe, F. J., & Flemming, R. L. (2013). Clay mineralogy, oxygen isotope geochemistry and water/rock ratio estimates, Te Mihi area, Wairakei Geothermal Field, New Zealand. *Clays and Clay Minerals*, *61*, 204–217. https://doi.org/10.1346/CCMN.2013.0610304

Lu, Z., Liu, Z., Chen, G., & Guan, J. (2019). Prominent precession-band variance in ENSO intensity over the last 300,000 years. *Geophysical Research Letters*, *46*, 9786–9795. https://doi.org/10.1029/2019GL083410

Magill, C. R., Ashley, G. M., & Freeman, K. H. (2013). Ecosystem variability and early human habitats in eastern Africa. *Proceedings of the National Academy of Sciences*, *110*(4), 1167–1174. https://doi.org/10.1073/pnas.1206276110

Moore, D., & Reynolds, R. Jr. (1997). *X-ray Diffraction and the identification and analysis of clay minerals*. Oxford, England: Oxford University Press.

Nicholson, S. E. (2018). The ITCZ and the seasonal cycle over equatorial Africa. *Bulletin of the American Meteorological Society*, *99*(2), 337–348. https://doi.org/10.1175/BAMS-D-16-0287.1

Ojiambo, B. S., Poreda, R. J., & Lyons, W. B. (2001). Ground water/surface water interactions in Lake Naivasha, Kenya, Using $\delta^{18}O$, δD, and $^3H/^3He$ age-dating. *Groundwater*, *39*(4), 526–533. https://doi.org/10.1111/j.1745-6584.2001.tb02341.x

Otte, I., Detsch, F., Mwangomo, E., Hemp, A., Appelhans, T., & Nauss, T. (2017). Multidecadal trends and interannual variability of rainfall as observed from five lowland stations at Mt. Kilimanjaro, Tanzania. *Journal of Hydrometeorology*, *18*(2), 349–361. https://doi.org/10.1175/JHM-D-16-0062.1

Post-Beittenmiller, D. (1996). Biochemistry and molecular biology of wax production in plants. *Annual review of Plant Biology*, *47*(1), 405–430. https://doi.org/10.1146/annurev.arplant.47.1.405

Rozanski, K., Araguas-Araguas, L., & Gonfiantini, R. (1996). *Isotope patterns of precipitation in the East African region: In T. C. Johnson, E. O. Odada (Eds.), The Limnology, climatology and paleoclimatology of the East African Lakes*, (p. 79–93). Gordon and Breach, Amsterdam.

Savin, S., & Lee, M. (1988). Isotopic studies of phyllosilicates. *In S.W. Bailey (Ed.), Hydrous Phyllosilicates.*, (pp. 189–223). Reviews in Mineralogy, 19. Mineralogical Society of America, Washington D.C.

Shi, Z., Liu, X., & Cheng, X. (2012). Anti-phased response of northern and southern East Asian summer precipitation to ENSO modulation of orbital forcing. *Quaternary Science Reviews*, *40*, 30–38. https://doi.org/10.1016/j.quascirev.2012.02.019

Simpson, A. M. (2016). Authigenic clays used as terrestrial climate proxies: Locality 80, Olduvai Gorge, Tanzania: M.Sc. thesis, Georgia State University, 141 p.

Skrzypek, G., Mydłowski, A., Dogramaci, S., Hedley, P., Gibson, J. J., & Grierson, P. F. (2015). Estimation of evaporative loss based on the stable isotope composition of water using Hydrocalculator. *Journal of Hydrology*, *523*, 781–789. https://doi.org/10.1016/j.jhydrol.2015.02.010

Timmermann, A., Lorenz, S. J., An, S. I., Clement, A., & Xie, S. P. (2007). The effect of orbital forcing on the mean climate and variability of the tropical Pacific. *Journal of Climate*, *20*(16), 4147–4159. https://doi.org/10.1175/JCLI4240.1

Trauth, M. H., Maslin, M. A., Deino, A., & Strecker, M. R. (2005). Late Cenozoic moisture history of East Africa. *Science*, *309*(5743), 2051–2053. https://doi.org/10.1126/science.1112964

Wynn, J. G. (2007). Carbon isotope fractionation during decomposition of organic matter in soils and paleosols: implications for paleoecological interpretations of paleosols. *Palaeogeography, Palaeoclimatology, Palaeoecology*, *251*(3-4), 437–448. https://doi.org/10.1016/j.palaeo.2007.04.009